Effect of lung inflation on pulmonary vascular resistance by arterial and venous occlusion

T. S. HAKIM, R. P. MICHEL, AND H. K. CHANG
Meakins-Christie and Lyman Duff Laboratories, Department of Physiology and Pathology, McGill University, Montreal, Quebec H3A 2B4, Canada

HAKIM, T. S., R. P. MICHEL, AND H. K. CHANG. *Effect of lung inflation on pulmonary vascular resistance by arterial and venous occlusion.* J. Appl. Physiol.: Respirat. Environ. Exercise Physiol. 53(5): 1110–1115, 1982.—To explain the changes in pulmonary vascular resistance (PVR) with positive- and negative-pressure inflation (PPI and NPI, respectively), we studied their effects in isolated canine left lower lobes perfused at constant flow rate. The venous pressure was kept constant relative to atmospheric pressure during lung inflation. The total arteriovenous pressure drop (ΔPt) was partitioned with the arterial and venous occlusion technique into pressure drops across arterial and venous segments (large indistensible extra-alveolar vessels) and a middle segment (small distensible extra-alveolar and alveolar vessels). PPI caused a curvilinear increase in ΔPt due to a large Starling resistance effect in the alveolar vessels associated with a small volume-dependent increase in the resistance of alveolar and extra-alveolar vessels. NPI caused an initial decrease in ΔPt due to reduction in the resistance of extra-alveolar vessels followed by an increase in ΔPt due to a volume-dependent increase in the resistance of all vessels. In conclusion, we provided for the first time evidence that lung inflation results in a volume-dependent increase in the resistance of both alveolar and extra-alveolar vessels. The data suggest that while the volume-related changes in PVR are identical with PPI and NPI, there are pressure-related changes that can be different between the two modes of inflation.

pulmonary circulation; positive-pressure inflation; negative-pressure inflation; alveolar and extra-alveolar vessels; dog

IT HAS BEEN SUGGESTED that, as the lung expands, alveolar vessels become longer and narrower and usually decrease their volume, whereas extra-alveolar vessels become longer and wider thereby increasing their volume (1, 7, 10, 12, 17, 19). However, since increases in length and in diameter of vessels both increase blood volume but have opposite effects on resistance, the change in pulmonary vascular resistance (PVR) during lung inflation cannot always be predicted from changes in blood volume. Most investigators (1, 3–5, 21) report that PVR rises gradually with positive-pressure inflation (PPI), whereas with negative-pressure inflation (NPI) PVR falls initially then rises gradually, so that a U-shaped curve results. The net change in total PVR with inflation has been attributed to a fall in the resistance of the extra-alveolar vessels and a rise in the resistance of the alveolar vessels (13, 22); there are, however, no direct measurements to support this contention.

Based on a Starling resistor model, Permutt (16) concluded that the observed differences between PPI and NPI can be eliminated if the PVR is related to transpulmonary pressure (Ptp) at constant vascular pressure relative to either airway pressure (PA) or pleural pressure (Ppl). It is believed (15, 23) that PA and Ppl are the pressures surrounding the alveolar and extra-alveolar vessels, respectively; but it has been difficult to assess their effects on these vessels principally because of the difficulty in measuring the resistance of the alveolar and extra-alveolar vessels separately. Therefore, it may be misleading to use either PA or Ppl as a reference for both types of vessels.

Previously (9), we used the arterial and venous occlusion technique to partition the PVR, under zone 3 conditions and at a small lung volume, into proximal arterial and distal venous segments separated by a distensible middle segment. In the present study, we used the same technique to measure the changes in the resistance of these three vascular segments with lung inflation. We found that there was a volume-dependent increase in the resistance of both alveolar and extra-alveolar vessels and that when calculating the resistance of these vessels in zone 2 conditions, their intravascular pressures should be referenced to PA and Ppl, respectively.

MATERIALS AND METHODS

Adult mongrel dogs (20–26 kg body wt) were anesthetized with pentobarbital sodium (25 mg/kg), intubated, and ventilated with a Harvard respirator. A thoracotomy was performed through the fourth left intercostal space. The left upper lobe was excised. Heparin (1,000 IU/kg) was administered intravenously. We dissected the left lower lobe (LLL) pulmonary artery, vein, and bronchus to prepare it for either in situ or in vitro isolated study (see below). In these two preparations we employed the arterial and venous occlusion technique (9) to partition the PVR as follows: at a steady and constant flow rate, we monitored the pulmonary arterial inflow pressure (Pa) and outflow venous pressure (Pv) from side ports in the arterial and venous cannulas. When the inflow into the arterial cannula was occluded suddenly, the Pa fell rapidly, then more slowly. Similarly at the same flow rate when the outflow from the venous cannula was occluded, the Pv rose rapidly and then more slowly. The duration of occlusion in both instances was 2–4 s. The rapid changes in Pa and Pv with inflow and outflow occlusion represented the respective pressure drops across the relatively indistensible arteries (ΔPa) and veins (ΔPv). A remaining pressure drop (ΔPm) across the middle disten-

sible vessels was calculated by subtracting the total arteriovenous pressure drop (ΔPt) − (ΔPa + ΔPv).

Positive-pressure inflation (PPI). In this group, we used an in situ LLL as previously described (9). With cannulas in the artery and vein, the LLL was perfused with a pump (Masterflex 7545) from a reservoir, and the outflow was drained from the vein into the same reservoir (Fig. 1*A*). The temperature of the perfusing blood was kept at 37°C. Through a divided tracheal tube, the LLL was ventilated with 5% CO_2-95% O_2 and the right lung with 100% O_2. The Pa was controlled by adjusting the flow rate, and Pv was set by the level of the reservoir. Pa, Pv, and LLL airway pressure (P_A) were measured with Statham transducers (PD23B) relative to the top of the LLL. The Pa and Pv signals were filtered with two identical flat-amplitude low-pass filters (Frequency Devices 744-PBI) with cutoff frequency set at 10 Hz, to eliminate the high-frequency artifacts generated by the perfusion pump, and recorded on an eight-channel Hewlett-Packard 7758B recorder.

Two sets of experiments were performed with PPI. *1*) In 11 dogs, Pv was set at 1.8 ± 0.2 (SE) Torr. With a constant flow of 558 ± 31 (SE) ml/min, the respirator to the LLL was stopped, and arterial occlusion (AO) and venous occlusion (VO), as previously described (9) and outlined above, were performed twice each at P_A levels of 0, 5, 10, 15, and 20 Torr by an overflow constant-pressure system. At each level of P_A, sufficient time was allowed for Pa to stabilize before AO and VO were performed. Ventilation was resumed for a few breaths between measurements. *2*) In six dogs, with the Pv set at 1.8 ± 0.1 Torr, the lobes were inflated to P_A = 15 Torr and were perfused at flow rates of 276 ± 15, 536 ± 32, and 800 ± 46 (SE) ml/min; at each flow rate AO and VO were performed as above.

Negative-pressure inflation (NPI). In this group, an in vitro isolated LLL preparation (Fig. 1*B*) was used. The LLL in seven dogs was excised, and cannulas were placed in the artery, vein, and bronchus. The lobe was perfused at a constant flow rate of 594 + 39 ml/min in a Plexiglas box in which negative pressure could be maintained. Pa and Pv were measured relative to the top of the lobe from side connectors in the cannulas, as with PPI. The lobe was ventilated with 5% CO_2-95% O_2, and Pv was set at 1.5 ± 0.4 Torr (zone 3). With the bronchus opened to the atmosphere, AO and VO were performed at different constant box pressures (Ppl) of 0, −5, −10, −15, and −20 Torr. AO and VO were repeated at the same pleural pressures when Pv was set at −5 or 10 Torr.

We have previously demonstrated that the in situ LLLs do not become edematous during the course of the experiment (9). We confirmed this in the isolated lungs of the present study and found that the wet-to-dry weight ratios of the isolated lobes at the end of the experiment [4.54 ± 0.20 (SD)] were not significantly different from the control values (4.78 ± 0.10) obtained at the beginning of the experiment from the left upper lobes of the same dogs. The results of this study are expressed as means ± SE.

RESULTS

Positive-pressure inflation. Figure 2 shows the effect of lung inflation by PPI on ΔPt, and on ΔPa, ΔPv, and ΔPm. As expected, ΔPt rose as Ptp increased. The slope of this curve was less than one at small lung volume and became larger than one at higher lung volume. ΔPa remained essentially unchanged, but ΔPv increased slightly as the lung was inflated. Thus the rise in ΔPt was mostly due to the increase in ΔPm. Increasing the flow rate at P_A = 15 Torr caused a linear rise in ΔPa and ΔPv (Table 1), suggesting that the arterial and venous segments acted as "true" resistances. In contrast, ΔPm fell slightly with increasing flow rate.

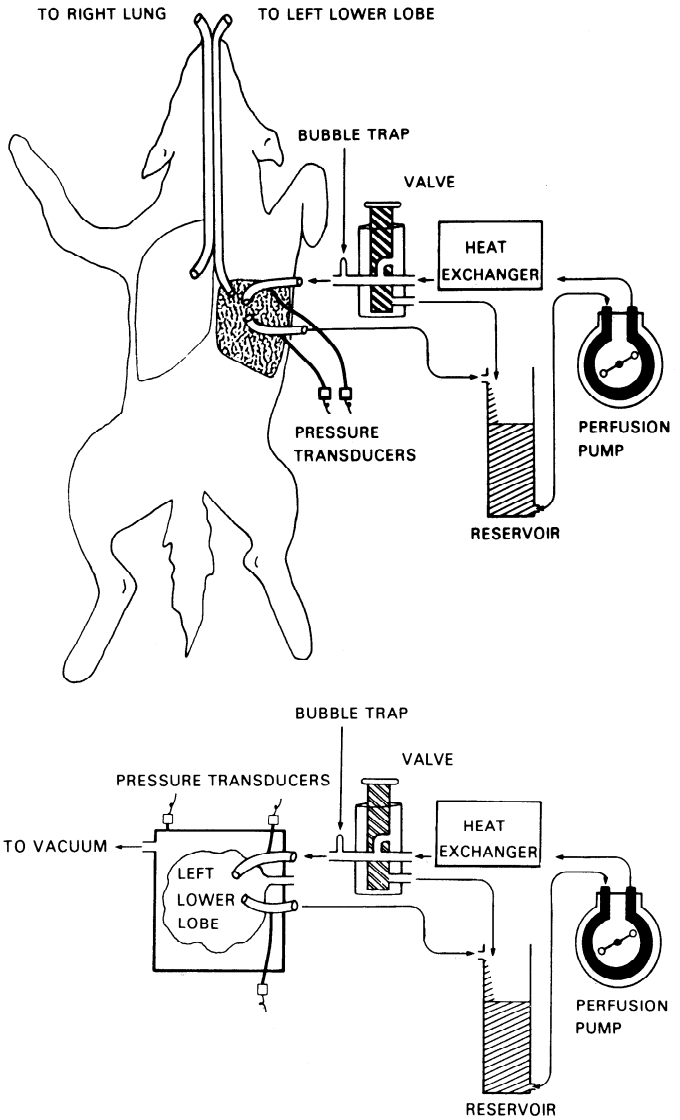

FIG. 1. *Top*: in situ left lower lobe preparation. *Bottom*: isolated left lower lobe preparation.

Negative-pressure inflation. With NPI of the lung at Pv of 1.5 Torr (zone 3), there was an initial fall in Pt that reached a minimum at Ptp of 5 Torr and then a gradual rise with continued inflation (Fig. 3). Because the flow rate was constant and the lung was in zone 3, the U-shaped curve of ΔPt vs. Ptp indicates a similar relationship exists between PVR and Ptp, as is usually observed (3, 21). Unexpectedly, however, the curves of the individual components of ΔPt, i.e., ΔPa, ΔPv, and ΔPm, were also U-shaped but less concave.

Figure 4 shows the relationship between Ptp and ΔPt,

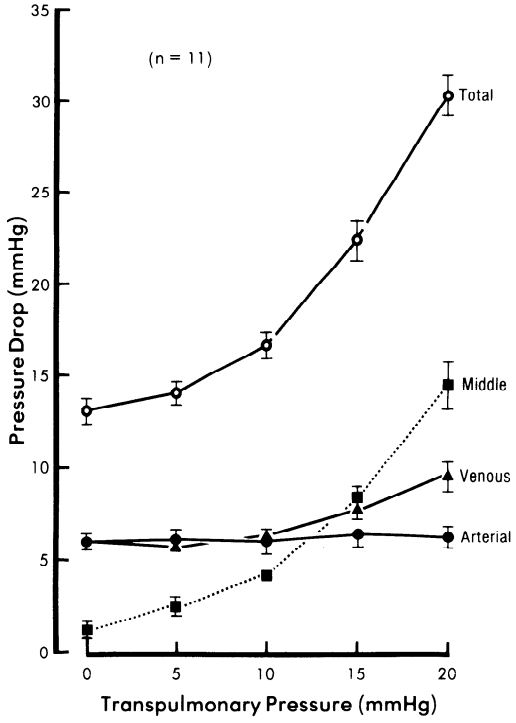

FIG. 2. Effects of transpulmonary pressure by positive-pressure inflation on total pressure drop (ΔPt) and on pressure drops across the arterial (ΔPa), venous (ΔPv), and middle (ΔPm) segments. Pleural pressure was atmospheric, and venous pressure was 1.8 Torr.

TABLE 1. *Effect of flow rate on distribution of pressure*

$\dot{Q}$, ml/min	P_A, Torr	ΔPt, Torr	ΔPa, Torr	ΔPv, Torr	ΔPm, Torr	$Pa' - P_A$, Torr
276	15	18.8 ± 0.8	4.5 ± 0.8	4.6 ± 0.4	10.1 ± 0.9	1.1
536	15	24.4 ± 1.1	7.7 ± 1.2	7.9 ± 0.6	9.4 ± 1.1	3.5
800	15	28.7 ± 1.2	9.6 ± 1.2	10.8 ± 0.8	8.8 ± 0.7	5.4

Values are means ± SE. See APPENDIX for definitions. $Pa' - P_A$ is the driving pressure in the middle segment.

ΔPa, ΔPv, and ΔPm at three different venous pressures. The U-shaped curve of ΔPt vs. Ptp (Fig. 4*A*) became less concave and shifted downward as Pv increased from −5 to 1.5 then to 10 Torr. This downward shift with elevation of Pv was due to a generalized increase in vascular pressure that distended the vessels at each lung volume. Figure 4*B* shows that the various levels of Pv had little effect on the shape and position of the curve describing ΔPa vs. Ptp. On the other hand, the curves describing ΔPm and ΔPv vs. Ptp were markedly altered by the level of Pv (Fig. 4, *C* and *D*). When Pv was −5 Torr and Ptp was 0, ΔPv increased probably because collapse of the large veins occurred as Ppl exceeded Pv throughout the lobe. The shape and positions of the curves of ΔPv vs. Ptp were otherwise only slightly affected by Pv. The U-shaped curve of ΔPm vs. Ptp was less concave and shifted downward as Pv increased from −5 to 10 Torr, as was the case with ΔPt (Fig. 4*C*).

Model of the pulmonary vasculature. Previous studies (8, 9) with the arterial and venous occlusion technique led us to conclude that the pulmonary vasculature consisted of two relatively indistensible (arterial and venous) segments separated by a highly distensible middle segment. The anatomic boundaries of each segment were not clearly defined, but the data suggested that the arterial and venous segments included small muscular vessels. The present data showed that airway pressure elevation increased ΔPm, which indicated that the middle segment contains at least alveolar vessels that collapse and form a Starling resistor when the alveolar pressure exceeds their intravascular pressure. If this Starling resistor effect occurred at the boundary between the middle and venous segments, the inflection point of Pv with venous occlusion should equal P_A when P_A is high, because the venous occlusion technique measures the pressure drop across all resistances downstream from the distensible region. However, we found that at high airway pressure, the inflection point was considerably lower than P_A, suggesting that there were distensible small veins between the Starling resistor and the indistensible venous segment. When the lung was perfused in a retrograde fashion (unpublished observations), similar results suggested there were also small distensible arteries. Therefore, the middle segment contains small distensible

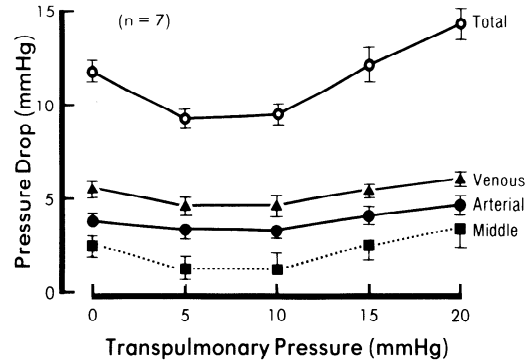

FIG. 3. Effects of transpulmonary pressure by negative-pressure inflation on total pressure drop (ΔPt) and on pressure drops across arterial (ΔPa), venous (ΔPv), and middle (ΔPm) segments. Airway pressure was atmospheric, and venous pressure was 1.5 Torr.

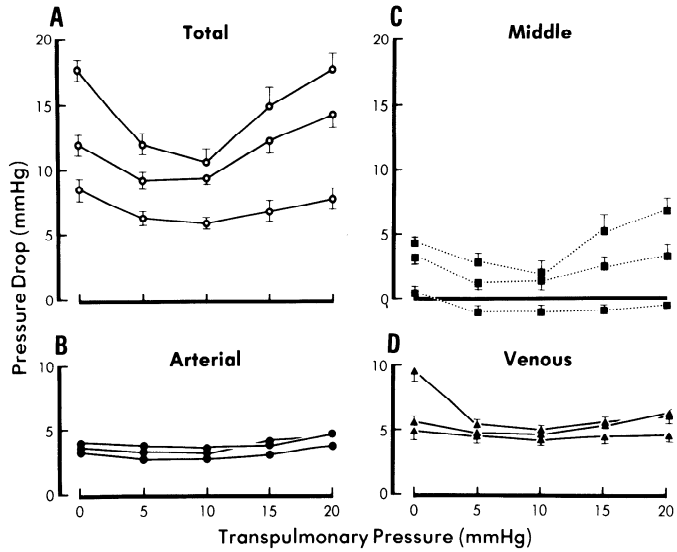

FIG. 4. Effect of negative-pressure inflation at different venous pressures on *A* (total), *B* (arterial), *C* (venous), and *D* (middle) pressure drops. In each *panel*, top curve was obtained at Pv = −5, middle curve at Pv = 1.5, and bottom curve of Pv = 10 Torr.

extra-alveolar arteries and veins in addition to the centrally located alveolar vessels. We constructed the model shown in Fig. 5 to further partition the pulmonary vasculature. In this model the pressures at the proximal and distal ends of the indistensible arterial segment (Pa and Pa′) and of the indistensible venous segment (Pv′ and Pv) could be obtained: Pa and Pv were measured directly, whereas Pa′ and Pv′ were calculated with the formulas $Pa' = Pa - \Delta Pa$ and $Pv' = Pv + \Delta Pv$. The relationship of the arterial, middle, and venous segments to alveolar and extra-alveolar vessels is also shown. The central portion of the middle distensible segment is made up of alveolar vessels that are presumably smaller than 30 μm in diameter (by definition collapse when PA exceeds both Pa and Pv) and more peripherally located small arteries and veins that are distensible but are extra-alveolar vessels. It is not clear if the alveolar vessels, including the capillaries, are distensible; however, since there is evidence to suggest that capillaries can be somewhat distensible (7) we lumped those alveolar vessels with other centrally located distensible extra-alveolar vessels. The arterial and venous segments are, on the other hand, made up of indistensible extra-alveolar vessels. The pressure surrounding the extra-alveolar vessels is primarily the pleural pressure, whereas the pressure surrounding the alveolar vessels is the alveolar pressure (15, 23).

DISCUSSION

With the arterial and venous occlusion technique, we had previously divided the lung vasculature into arterial and venous segments separated by a middle segment (9). Under zone 3 conditions and at small lung volume, the arterial and venous segments were major sites of resistance, whereas the middle segment was the major site of compliance. The resistance of the arterial and venous segments was unaffected by their intravascular pressure when it exceeded Ppl by 15 and 5 Torr, respectively. In addition we demonstrated that the resistance of the middle segment became negligible when its intravascular pressure exceeded PA by about 12 Torr (9).

In the present study, we measured the changes in pressure drops of ΔPa, ΔPm, and ΔPv segments with lung inflation. We found that with both PPI and NPI, there were volume-dependent increases in ΔPa, ΔPm, and ΔPv. Because the blood flow was constant, the vascular pressures changed relative to PA or Ppl with inflation and had pressure-related effects on ΔPa, ΔPm, and ΔPv in addition to the volume-related effects; i.e., with PPI (Fig. 2), ΔPm increased further because the vascular pressure in the middle segment decreased relative to PA (Starling resistor effect); and with NPI (Fig. 3), there was a small initial decrease in ΔPa and ΔPv because Pa and Pv increased relative to Ppl, thereby distending the arterial and venous segments.

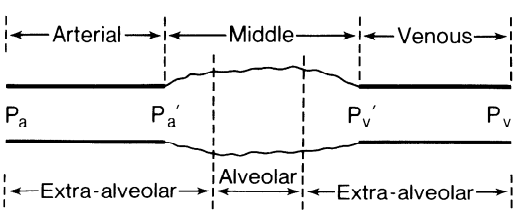

FIG. 5. A model of pulmonary vasculature relating arterial, middle, and venous segments to alveolar and extra-alveolar vessels (see text).

The results of our study enabled us to further partition the pulmonary vasculature into alveolar and extra-alveolar vessels (Fig. 5). In this model, ΔPm measures the total pressure drop in both the alveolar and small extra-alveolar vessels of the middle segment. The contribution of the small distensible extra-alveolar vessels to ΔPt is small in zone 3 and became even smaller as they distend by increasing their pressure relative to Ppl. Therefore, ΔPm measures mainly the pressure drop in the alveolar vessels. Similarly, ΔPa and ΔPv measured the pressure drops across the extra-alveolar arteries and veins, respectively.

The effects of PPI and NPI on the alveolar and extra-alveolar vessels can be understood accurately if we consider the effects of lung volume and of intravascular pressure relative to PA and Ppl on each segment, PA and Ppl being the pressure surrounding the alveolar and extra-alveolar segments, respectively (15, 23). The pulmonary compliance curve indicates that an increase in Ptp from 0 to 10 Torr results in a small increase in lung volume, whereas an increase in Ptp from 10 to 20 Torr results in a large volume increase (6). During inflation, the lengthening of all vessels tends to increase their resistance; in addition, however, extra-alveolar vessels may distend radially due to their interdependence with the lung parenchyma and may decrease their resistance (2, 10, 12, 19). With PPI, we observed a small increase in ΔPv between Ptp of 10–20 Torr (Fig. 2), which was probably due to the predominant effect of lengthening over radial interdependence. While a similar effect would be expected on the arterial side, ΔPa did not change because of the large increase in Pa relative to Ppl. However, we cannot exclude the possibility that the difference in the changes between ΔPa and ΔPv were also due to a stronger interdependence between the lung parenchyma and the arteries than between the parenchyma and the veins (2, 11, 19). The large increase in ΔPm observed with PPI was mostly due to the formation of a Starling resistor in the alveolar vessels. However, the increase in Pa′, the pressure at the upstream end of the middle segment (Fig. 4) relative to PA, suggests that in addition to the Starling resistor, the "true" resistance of the middle segment had also increased with inflation, presumably due to the lengthening of its vessels. This was further supported by the fact that when PA was constant at 15 Torr, Pa′ increased with flow rate (Table 1).

With NPI, as with PPI, the lung volume and volume-dependent changes would be expected to be small between Ptp of 0 and 10 Torr. Initially, the increase in Pa and Pv relative to Ppl predominated over the effect of lengthening and resulted in a small fall of ΔPa and ΔPv (Fig. 3). Inflation beyond a Ptp of 10 Torr produced a volume-dependent increase in ΔPa and ΔPv due to the predominant effect of lengthening because the arterial and venous segments do not distent more by further increase in their pressure relative to Ppl (9, 11). The small initial decrease in ΔPm during NPI (Fig. 3) may have been due to distension of the small extra-alveolar vessels in the middle segment because their pressure increased relative to Ppl. With further inflation, in spite

of a continuing increase in vascular pressure relative to Ppl, ΔPm increased due to a volume-dependent lengthening of the alveolar vessels. This suggests that a change in Ppl has little effect on the alveolar vessels. In summary on the basis of the changes observed in ΔPa, ΔPv, and ΔPm it appears that PPI and NPI produce identical small volume-dependent increases in the resistance of both alveolar and extra-alveolar vessels. Furthermore, any difference in the changes in ΔPa, ΔPv, and ΔPm with PPI and NPI apparently result from a difference in the transmural pressure that develops across these segments.

In our preparation lung inflation caused the vascular pressure to change differently relative to PA and Ppl in each of the three vascular segments, and therefore we would not expect identical changes in total PVR with PPI and NPI. Thus while the volume-related changes in PVR were identical with PPI and NPI, the pressure-related changes in PVR were not identical.

The distribution of pressure drops in zone 2 conditions (Fig. 2) should be interpreted with caution, since other zone 2 conditions can exist whereby a large pressure drop can occur in the venous segment (14) due to collapse of the large veins (18, 20, 23, 24). The contribution of each segment of the pulmonary vasculature to the total pressure drops in zone 2 depends on whether Pv is less than Ppl, in which case the large veins would collapse and ΔPv rises (Fig. 4*D*), or whether Pv is less than PA but larger than Ppl, in which case ΔPm rises. When the large veins collapse, any reduction of Pv would have little effect on the alveolar vessels, whereas if the large veins do not collapse, a reduction in Pv will decrease the pressure in the alveolar vessels relative to PA and increase ΔPm (Fig. 4*C*). The latter condition is identical to what happens in the intact lung, for example, on taking a deep breath, Pa and Pv remain essentially constant relative to Ppl but fall relative to PA, and therefore a large fraction of the pressure drop would occur in the alveolar vessels as with PPI.

The total PVR is usually calculated with the equation $(Pa - Pv)/\dot{Q}$, where $\dot{Q}$ is the flow rate. In zone 2 conditions, flow is independent of Pv, and the back pressure becomes PA. Therefore, it has been suggested that PVR in zone 2 be calculated with Pa − PA as the driving pressure (16). In this case, however, the resistance of vessels downstream from the alveolar vessels is not accounted for. Thus it is misleading to compare PVR values calculated in zone 3 with those calculated in zone 2 because these calculated values measure the resistances of different segments of the vasculature. Our data allowed us to circumvent this problem by comparing the sum of the resistances of the individual segments. To do this, we used Pa − Pa′ as the driving pressure in the arterial segment and Pa′ − Pv′ or Pa′ − PA as the driving pressures in the middle segment in non-Starling and in Starling conditions, respectively, and Pv′ − Pv or Pv′ − Ppl as the driving pressures in the venous segment when the large veins are in noncollapsed and in collapsed conditions, respectively. When we did this, we found that the PVR increased by 50–60% with full inflation; if Pa − Pv or Pa − PA were used as driving pressures, marked differences in calculated PVR in zone 2 and 3 would result.

In conclusion we have examined the effects of lung inflation on the resistances of the arterial, venous, and middle segments and of alveolar and extra-alveolar vessels. Inflation caused a small but consistent volume-dependent increase in the resistances of alveolar and extra-alveolar vessels. The curvilinear increase in ΔPt with PPI was attributed to a Starling resistor formation in the alveolar vessels associated with volume-dependent increases in the resistance of the alveolar and extra-alveolar vessels. The U-shaped relationship of ΔPt vs. Ptp with NPI was attributed to an initial pressure-related decrease in the resistance of the extra-alveolar vessels associated with a volume-dependent increase in the resistance of the alveolar and extra-alveolar vessels. The concavity of the U-shaped curve of ΔPt with NPI was attenuated by venous pressure elevation. By studying the effects of PPI and NPI, we found blood vessels in the middle segment (alveolar vessels) influenced primarily by changes in their pressure relative to PA and vessels in the arterial and venous segments (extra-alveolar vessels) influenced by their pressure relative to Ppl. These results have direct bearing on the calculation of PVR in zone 3 and zone 2 conditions during inflation. Any apparent differences between the effects of PPI and NPI are due to differences in the transmural pressure that develops across the alveolar and extra-alveolar vessels.

APPENDIX

Pa	pulmonary arterial pressure of LLL
Pv	pulmonary venous pressure of LLL
ΔPt	total arteriovenous pressure drop (Pa − Pv)
ΔPa	pressure drop in the arterial segment (from arterial occlusion)
ΔPv	pressure drop in the venous segment (from venous occlusion)
ΔPm	pressure drop in the middle segment (ΔPt − ΔPa − Pv)
Pa′	pressure in the distal end of the arterial segment (Pa − ΔPa)
Pv′	pressure in the proximal end of the venous segment (Pv + ΔPv)
PA	airway or alveolar pressure
Ppl	pleural or box pressure
Ptp	lung transpulmonary pressure (PA − Ppl)
PVR	pulmonary vascular resistance
PPI	positive-pressure inflation
NPI	negative-pressure inflation
$\dot{Q}$	flow rate

The authors thank Timothy Smith for his technical assistance.

This work was suppported by National Heart, Lung, and Blood Institute Grant HL-24348 and by the Medical Research Council of Canada Grants MA-7046 and MA-6474.

Received 21 September 1981; accepted in final form 14 June 1982.

REFERENCES

1. BANISTER, J., AND R. W. TORRANCE. The effects of the tracheal pressure upon flow: pressure relations in the vascular bed of isolated lungs. *Q. J. Exp. Physiol.* 45: 352–368, 1960.
2. BENJAMIN, J. J., P. S. MURTAGH, D. F. PROCTOR, H. A. MENKES, AND S. PERMUTT. Pulmonary vascular interdependence in excised dog lobes. *J. Appl. Physiol.* 37: 887–894, 1974.
3. DAWSON, C. A., D. J. GRIMM, AND J. H. LINEHAN. Effects of lung inflation on longitudinal distribution of pulmonary vascular resistance. *J. Appl. Physiol.: Respirat. Environ. Exercise Physiol.* 43: 1089–1092, 1977.
4. DAWSON, C. A., R. L. JONES, AND L. H. HAMILTON. Hemodynamic responses of isolated cat lungs during forward and retrograde per-

fusion. *J. Appl. Physiol.* 35: 95–102, 1973.
5. DeBono, E. F., and C. G. Caro. Effect of lung-inflating pressure on pulmonary blood pressure and flow. *Am. J. Physiol.* 205: 1178–1186, 1963.
6. Glaister, D. H., R. C. Schroter, M. F. Sudlow, and J. Milic-Emili. Bulk elastic properties of excised lungs and the effects of transpulmonary pressure gradient. *Respir. Physiol.* 17: 347–364, 1973.
7. Glazier, J. B., J. M. B. Hughes, J. E. Maloney, and J. B. West. Measurement of capillary dimension and blood volume in rapidly frozen lungs. *J. Appl. Physiol.* 26: 65–76, 1969.
8. Hakim, T. S., C. A. Dawson, and J. H. Linehan. Hemodynamic responses of dog lung lobe to lobar venous occlusion. *J. Appl. Physiol.: Respirat. Environ. Exercise Physiol.* 47: 145–152, 1979.
9. Hakim, T. S., R. P. Michel, and H. K. Chang. Partitioning of pulmonary vascular resistance in dogs by arterial and venous occlusion. *J. Appl. Physiol.: Respirat. Environ. Exercise Physiol.* 52: 710–715, 1982.
10. Howell, J. B. L., S. Permutt, D. F. Proctor, and R. L. Riley. Effect of inflation of the lung on different parts of the pulmonary vascular bed. *J. Appl. Physiol.* 16: 71–76, 1961.
11. Lai-Fook, S. J. A continuum mechanic analysis of pulmonary vascular interdependence in isolated dog lobes. *J. Appl. Physiol.: Respirat. Environ. Exercise Physiol.* 46: 419–429, 1979.
12. Macklin, C. Evidence of increase in the capacity of the pulmonary arteries and veins of dogs, cats and rabbits during inflation of the freshly excised lung. *Rev. Can. Biol.* 5: 199–232, 1946.
13. Murray, J. F. *The Normal Lung.* Philadelphia, PA: Saunders, 1976, p. 131.
14. Parker, J. C., R. E. Parker, D. N. Granger, and A. E. Taylor. Vertical gradient in regional vascular resistance are pre to post resistance ratios in the dog lung. *Lymphology* 12: 191–200, 1979.
15. Permutt, S. Mechanical influences on water accumulation in the lungs. In: *Pulmonary Edema*, edited by A. P. Fishman and E. M. Renkin. Washington, DC: Am. Physiol. Soc., 1979, p. 175–194.
16. Permutt, S., B. Bromberger-Barnea, and H. N. Bane. Alveolar pressure, pulmonary venous pressure and vascular waterfall. *Med. Thorac.* 19: 239–260, 1962.
17. Roos, A., L. J. Thomas, E. L. Nagel, and D. C. Prommas. Pulmonary vascular resistance as determined by lung inflation and vascular pressures. *J. Appl. Physiol.* 16: 77–84, 1961.
18. Smith, H. G., and J. Butler. Pulmonary venous waterfall and perivenous pressure in the living dog. *J. Appl. Physiol.* 38: 304–308, 1975.
19. Smith, J. C., and W. Mitzner. Analysis of pulmonary vascular interdependence in excised dog lobes. *J. Appl. Physiol.: Respirat. Environ. Exercise Physiol.* 48: 450–467, 1980.
20. Takahashi, S., and J. Butler. A vascular waterfall in extra-alveolar vessels of the excised dog lung. *J. Appl. Physiol.* 26: 578–584, 1969.
21. Thomas, L. J., Z. J. Griffo, and A. Roos. Effect of negative pressure inflation of the lung on pulmonary vascular resistance. *J. Appl. Physiol.* 16: 451–456, 1961.
22. West, J. B. *Respiratory Physiology.* Baltimore, MD: Williams & Wilkins, 1979, p. 39.
23. West, J. B., and C. T. Dollery. Distribution of blood flow and the pressure-flow relations of the whole lung. *J. Appl. Physiol.* 20: 175–183, 1965.
24. Whittenberger, J. L., M. McGregor, E. Berglund, and H. G. Borst. Influence of state of inflation of the lung on pulmonary vascular resistance. *J. Appl. Physiol.* 15: 878–882, 1960.